Modification of 3D active wheel surface structure

Modyfikacja struktury przestrzennej czynnej powierzchni ściernicy (CPS)

DOI: https://doi.org/10.17814/mechanik.2017.10.141

RAFAŁ ŚWIERCZ
JÓZEF ZAWORA
LUCJAN DĄBROWSKI
MIECZYSŁAW MARCINIAK *

The investigation has been carried out into the effect of modifying the active wheel surface (AWS) structure in view of enhancing productivity of the grinding process. This undertaking should be consistent with standard surface roughness requirements. This modification involves the model-based shares of the two SiC grain grit numbers and two CrA (corundum with chromium addition) grit numbers in the grinding pins with ceramic bond for the face grinding process.
KEYWORDS: planar grinding, wheel with different grit ~~size~~ number, gumming, material removal rate

Modern methods of intensification of the grinding process depend largely on increasing wear resistance of the grains constituting properly developed AWS profile [1]. Further advances in this field are evident in the research and production of hybrid wheels with a mixture of CBN grains and grinding wheels with aggregate grains, as well as in the use of microcrystalline grains. Modified AWS structure is based on the view that the evaluation of the working conditions of the isolated micro-cutting edge can not be the basis for describing the machining efficiency of the whole tool such as a grinding wheel. The actual profile of active surface of the grinding wheel in the grinding conditions specifies limits or expands the amount of contact of the adhesive surface of the workpiece and promotes or prevents from pasting the ground surface material into the AWS. Under traditional circumferential longitudinal grinding conditions, only part of the AWS participates in intensive material removal and the next part performs finishing work with a significant proportion of the binder. This natural variation in geometrical grinding conditions was the basis for the construction of a multi-layer grinding wheel with different grain granulation in the individual layers (fig. 1).

The grinding wheel of such a structure has the largest grains in the first layer at the longitudinal feed direction. Structural construction of this layer allows for intensive processing and, due to the increased grain spacing, limits the potential negative effect of the AWS. This is illustrated by comparison of grinding forces (F_n normal and tangential F_t) during grinding using the conventional and multi-layered grinding wheel (fig. 2).

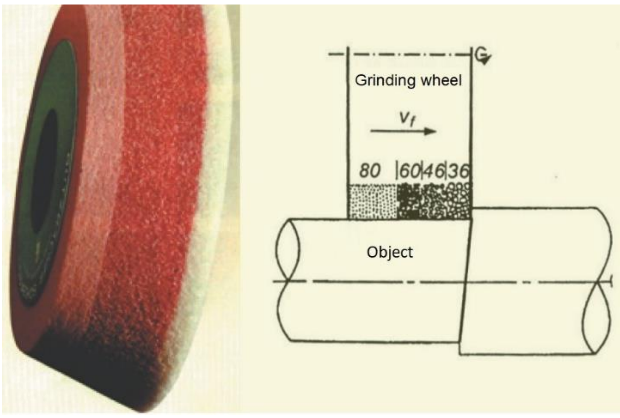

Fig. 1. Example of multilayer grinding wheel (left) and peripheral grinding principle with 4-layer grinding wheel with grains with granulation numbers: 36, 46, 60, 80 [2, 3]

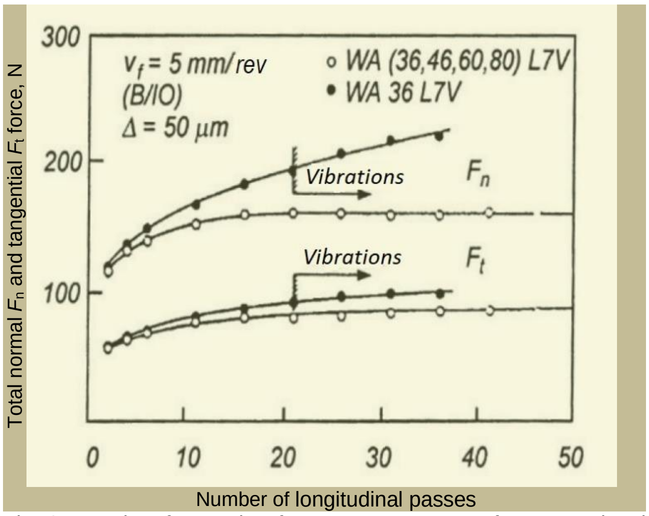

Fig. 2. Results of F_n and F_t forces measurements for conventional grinding wheel WA 36 L7V and multi-layered WA (36, 46, 60, 80) L7V

In the case of conventional grinding, only 20 passes have been recorded in the machining system, indicating AWS dullness. While at work of multilayered grinding wheel, the phenomenon has not occurred even after 50 machining passes.

Research program

For comparing the face grinding results with CrA36L7V and SiC36L7V grinding wheels, the modified AWS grinding wheels were used, which in both cases included mixture of grains with a grit number 36 and 80 (fig. 3).

* Dr inż. Rafał Świercz (rsw@meil.pw.edu.pl); dr hab. inż. Józef Zawora (jzawora@meil.pw.edu.pl); dr hab. inż. Lucjan Dąbrowski, prof. nadzw. (ld@meil.pw.edu.pl); dr hab. inż. Mieczysław Marciniak, prof. nadzw. (mima@meil.pw.edu.pl) – Politechnika Warszawska

Fig. 3. Grinding wheels with the modified structure of SiC and CrA grains

In the modified grinding wheels, the standard percentage of abrasive *Vz* is maintained, which for medium grade *L* and structure number 7 is 48%. This standard proportion of abrasives consists of an experimentally adjusted percentage of grains with a grit number 36 and smaller grains with a grit number 80 in the following volume proportions:

$$Vz = 50\%\,Vz_{36} + 50\%\,Vz_{80}$$

In the modified $CrA_{(m)}$ and $SiC_{(m)}$ grinding wheels (fig. 3), the standard proportion of the binder was retained, resulting in a reduction in the average cross-section of the bridges [4, 5].

For face grinding, a surface grinder with hydraulic feed drive and a rotating spindle with a rotational speed of n = 16,000 rpm was used (fig. 4).

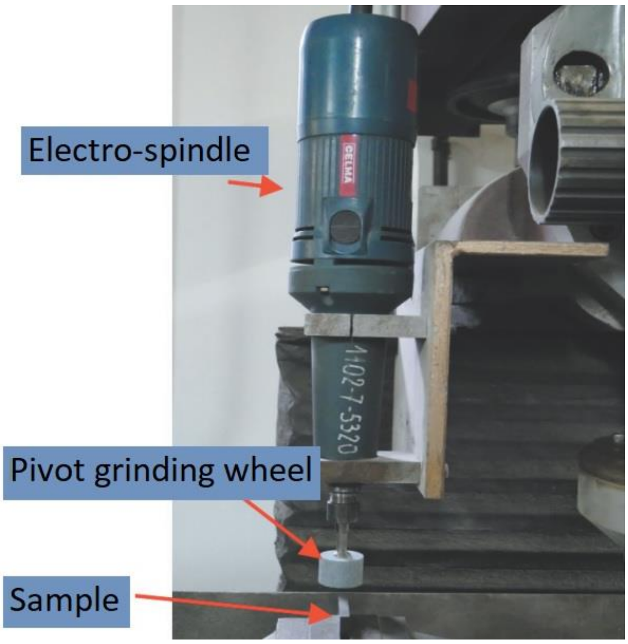

Fig. 4. Position for the face grinding efficiency tests

Comparative studies of machining efficiency of conventional and modified grinding wheels were carried out by means of indirect measurements of the indicator *q*, i.e. the AWS gumming level, recorded on the instrument shown in fig. 5, and by measurement of the material removal in subsequent grinding time periods.

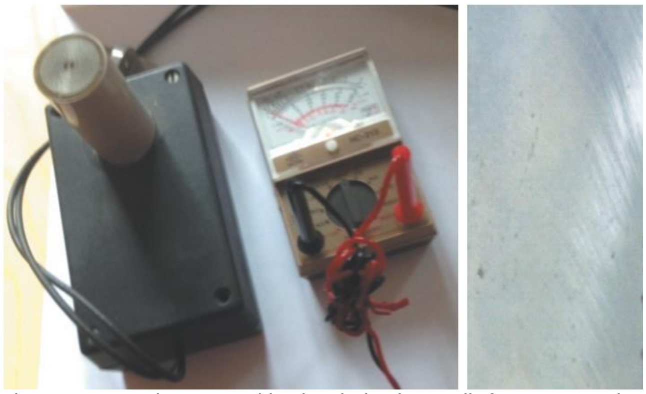

Fig. 5. Measuring set with the induction coil for comparative evaluation of metal mass gumming the AWS (left) and ground surface appearance

Results

In the table, arbitrary indicators *q* characterizing the susceptibility of the active surface of tested SiC and CrA grain wheels with standard and modified structure, were listed: $CRA_{(m)}$ and $SiC_{(m)}$.

TABLE. Arbitrary indicators *q(mA)* of AWS gumming degree with ground steel 100Cr

Tool	Standard grinding wheels		Modified grinding wheels	
	SiC	CrA	$SiC_{(m)}$	$CrA_{(m)}$
Grain granulation	36 80	36 80	(36+80)	(36+80)
Gumming indicator *q*(mA)	4 6	3 4,5	3,5	2,8

Comparison of arbitrary *q* degree of the AWS gumming in the case of standard grinding wheels confirms the role of chemical affinity, which increases susceptibility to gumming of the grinding wheels with SiC grains relative to the grinding wheels with CrA grains – regardless of the size of these grains. The quantitative results of the grinding performance of standardized grinding wheels are presented in fig. 6. Grinding wheels with standard grains CrA, grit No. 36 and grains SiC, grit No. 36 are more efficient (curves 1 and 3 in fig. 6) than the wheels with CrA, grit No. 80 and wheels SiC, grit No. 80 (curves 2 and 4 in fig. 6). These differences are due to the different conditions of micro-cutting with grains of different granulation and greater susceptibility to the active surface of grinding wheels with grains of grit No. 80. In the modified AWS structures, i.e. $CrA_{(m)}$ and $SiC_{(m)}$, the presence of fine grains results in changing the contact conditions of the grinding wheel with ground material, as it creates locally a spatial structure having the properties of microcrystalline grains. This structure is reproduced after each dressing operation, so that the grinding process will involve grains No. 36 and 80.

This way of removing the machining allowance gives better results in terms of grinding performance for the modified AWS grinding wheels with the same operating parameters. This is illustrated by the obtained quantitative results regarding the grinding performance with both $CrA_{(m)}$ (curve 1 in fig. 7) and $SiC_{(m)}$ (curve 2 in fig. 7).

The results obtained for the performance of $CrA_{(m)}$ grinding wheels show that they are better than $SiC_{(m)}$ grinding wheels , wherein these resulting values are still higher– by 50÷80% – than the values achieved for standard grinding wheels. The improvement of the grinding performance is possible due to the reduced cross-section of the bond bridges. This is caused by the increased share of grains with grit number 80 in the grinding wheel volume. The modified 3-d structure of the AWS supports the crush-dressing process, which is facilitated by the thin bridges of

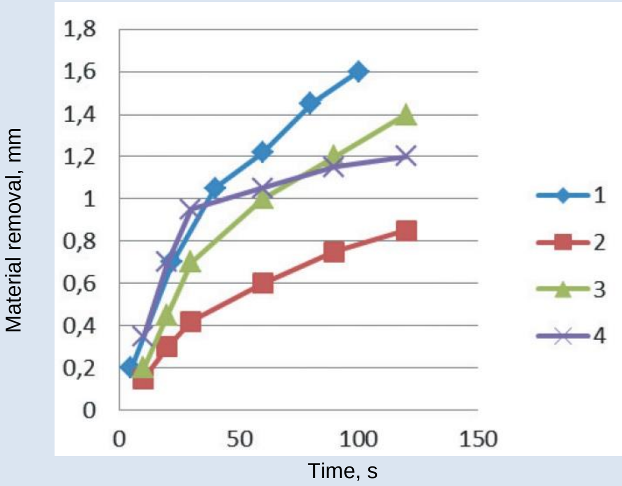

Fig. 6. Grinding performance with standard grinding wheels with CrA grains, grit No. 36 and 80 (curves 1 and 3) and with SiC grains, grit No. 36 and 80 (curves 2 and 4)

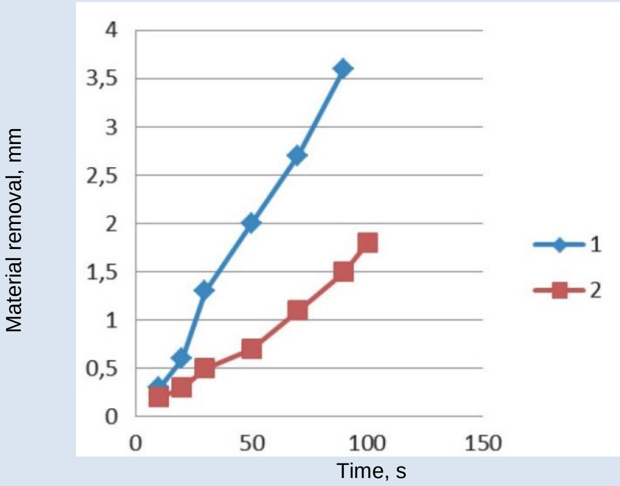

Fig. 7. Performance of the face grinding using grinding wheels with modified $CrA_{(m)}$ structure (curve 1) and $SiC_{(m)}$ grinding wheel (curve 2)

the binder. Moreover, the share of grains with grit number 80 in modified wheels promotes intensification of removing the fractures.
caused by the increased share of grains with grit number 36 in the grinding wheel volume. The major advantages of the tested grinding wheels are the reduction of grinding forces and the prolongation of the working time between successive dressings.

Conclusions

In the face grinding, the vertices of the abrasive grains move in the microcirculation zone along the complex cycloidal curve. The practical conditions for the destruction of the ground metal layer are, in this case, dependent on the 3-d structure of the grinding wheel surface. Modeling of the structure and its contact with the machined surface clearly indicate an active role of only 5 percent share of the grain volume.

Machining efficiency of collection of grains in the AWS, as assessed in terms of stochastic process, depends on the dimensions, the angles of the corners and the flatness of the walls of these grains [6]. This effect is also influenced by the size and uniformity of the distribution of the pores in the volume of the grinding wheel. This is achieved by modifying the AWS structure by applying granules of different granularity, which is a physical justification for the possibility of their efficient use in technology. This was confirmed by the results of the research process and the results of the AWS blockages grinding performance. The latter was influenced by the superposition of the effects of the larger size (# 36) graining process and the smaller grafts (number 80), which simultaneously play a decisive role in achieving the required stereometry of the grinding surface that is obtainable in the grinding process. This applies in particular for grinding wheels with the latest variant grains of aluminum nitride-oxide (AlON), which can be used for grinding steel with a hardness of 45 to 60 HRC and stainless steel. These grains are very useful in grinding processes, for which a large contact surface of the grinding wheel with a ground part is typical and which is subject to the risk of thermal damage to the workpiece. The following processes belong to this category [7, 8]:

- grinding with grinders of vertical axis,
- plunge grinding,
- creep feed grinding,
- centerless grinding,
- grinding of crankshafts.

The observed reduction of the active area of the grinding wheel results in an additional reduction of thermal loads in the grinding zone.

REFERENCES

1. Koziarski A. „*Czynna powierzchnia ściernicy*". Łódź: Wydawnictwo Naukowe Politechniki Łódzkiej, 1997.
2. Nadolny K., Plichta J. „*Jednoprzejściowe szlifowanie otworów ściernicami o strefowo zróżnicowanej budowie*". Praca zbiorowa. Koszalin: Wydawnictwo Uczelniane Politechniki Koszalińskiej, 2008.
3. Nakajima T., Okamura K., Uno Y. "Traverse grinding techniques for improving both productivity and surface finish". *International Grinding Conference*, Fontana, Wisconsin. SME, Mr84-534, August 27–29, 1984.
4. Olszak W. „*Obróbka skrawaniem*". Warszawa: WNT, 2008.
5. Niżankowski Cz. „*Technologia i eksploatacja ściernic z korundów spiekanych stosowanych w procesach szlifowania płaszczyzn*". Kraków: Wydawnictwo Politechniki Krakowskiej, 2013.
6. Kacalak W., Szafraniec F. Tandecka K. „Metodyka modelowania powierzchni czynnej narzędzi ściernych z uwzględnieniem korelacji przestrzennego rozmieszczenia ich wierzchołków dla określonych ściernic rzeczywistych". *Mechanik.* 8–9 (2014): pages 185.
7. Oczoś K.E., Habrat W. „Innowacje w obróbce ściernej. Cz. I. Ściernice, szlifierki uniwersalne i produkcyjne". *Mechanik.* 11 (2008): pages 895.
8. Świercz R., Oniszczuk-Świercz D., Dąbrowski L. „Mikroobróbka wykończeniowa – obróbka przetłoczno-ścierna. *Mechanik.* 8–9 (2016): pages 1132–1133.